Everolimus Reduces ^{89}Zr-Bevacizumab Tumor Uptake in Patients with Neuroendocrine Tumors

Sophie J. van Asselt[1,2], Sjoukje F. Oosting[1], Adrienne H. Brouwers[3], Alfons H.H. Bongaerts[1,4], Johan R. de Jong[3], Marjolijn N. Lub-de Hooge[3,5], Thijs H. Oude Munnink[1], Helle-Brit Fiebrich[1], Wim J. Sluiter[2], Thera P. Links[2], Annemiek M.E. Walenkamp[1], and Elisabeth G.E. de Vries[1]

[1]Department of Medical Oncology, University of Groningen, University Medical Center Groningen, Groningen, The Netherlands; [2]Department of Endocrinology, University of Groningen, University Medical Center Groningen, Groningen, The Netherlands; [3]Department of Nuclear Medicine and Molecular Imaging, University of Groningen, University Medical Center Groningen, Groningen, The Netherlands; [4]Department of Radiology, University of Groningen, University Medical Center Groningen, Groningen, The Netherlands; and [5]Department of Hospital and Clinical Pharmacy, University of Groningen, University Medical Center Groningen, Groningen, The Netherlands

Everolimus increases progression-free survival in patients with advanced neuroendocrine tumors (NETs). Currently, no biomarkers are available for early selection of patients who will benefit from everolimus. Everolimus can reduce vascular endothelial growth factor A (VEGF-A) production by tumor cells. Therefore, we aimed to investigate the effect of everolimus on tumor uptake of the radioactive-labeled VEGF-A antibody bevacizumab with PET in NET patients. **Methods:** Patients with advanced progressive well-differentiated NETs underwent ^{89}Zr-bevacizumab PET scans before and at 2 and 12 wk during everolimus treatment. ^{89}Zr-bevacizumab uptake was quantified by the maximum standardized uptake value (SUV_{max}). Tumor response and the percentage change in the sum of target lesion diameters were determined according to Response Evaluation Criteria in Solid Tumors 1.1 on CT (3 monthly). **Results:** In 4 of the 14 patients entered, no tumor lesions were visualized with ^{89}Zr-bevacizumab PET. In the remaining patients, 19% of tumor lesions 1 cm or greater known by CT were visualized. Tumor SUV_{max} decreased during everolimus treatment, with a median of −7% at 2 wk ($P = 0.09$) and a median of −35% at 12 wk ($P < 0.001$). The difference in SUV_{max} at 2 and 12 wk with respect to SUV_{max} at baseline correlated with percentage change on CT at 6 mo ($r^2 = 0.51$, $P < 0.05$, and $r^2 = 0.61$, $P < 0.01$, respectively). **Conclusion:** This study demonstrates variable ^{89}Zr-bevacizumab PET tumor uptake in NET patients. ^{89}Zr-bevacizumab tumor uptake diminished during everolimus treatment. Serial ^{89}Zr-bevacizumab PET might be useful as an early predictive biomarker of anti–VEGF-directed treatment in NET patients.

Key Words: neuroendocrine tumors; ^{89}Zr-bevacizumab PET; VEGF-A; everolimus; biomarker

J Nucl Med 2014; 55:1087–1092
DOI: 10.2967/jnumed.113.129056

Angiogenesis is a hallmark for tumor growth and for development of metastases (*1*). Vascular endothelial growth factor A (VEGF-A) produced by tumors is one of the main factors responsible for angiogenesis. Currently, several antiangiogenic therapies are available as anticancer agents, including VEGF-A antibodies, tyrosine kinase inhibitors, and mammalian target of rapamycin (mTOR) inhibitors. Antiangiogenic drugs are of interest in patients with well-differentiated neuroendocrine tumors (NETs) (*2*) because these tumors are hypervascular (*3–6*). mTOR indirectly stimulates angiogenesis but also induces messenger RNA translation of other genes important for cell survival and proliferation (*7*).

Phase 3 trials have shown superior progression-free survival in patients with advanced well-differentiated NETs treated with the VEGF receptor tyrosine kinase inhibitor sunitinib or the mTOR inhibitor everolimus. Compared with placebo, sunitinib resulted in a progression-free survival benefit of 5.9 mo in pancreatic NET (pNET) patients (*8*). Two trials with everolimus, 1 in pNET patients and 1 in patients with NETs associated with carcinoid syndrome, showed a progression-free survival benefit of 6.4 and 5.1 mo, respectively, in favor of everolimus, compared with placebo (*9,10*).

Because not all patients benefit from everolimus, biomarkers to select patients who will profit from treatment would be extremely helpful. An attractive candidate is VEGF-A. mTOR inhibition reduced VEGF-A excretion by NET cell lines (*11*). Additionally, in renal cancer xenografts, sensitivity to mTOR inhibition correlated with reductions in tumor hypoxia-inducible factor 1α messenger RNA translation, VEGF-A expression, and angiogenesis (*12*). However, circulating VEGF-A in patients treated with antiangiogenic drugs has not yet shown a clear predictive value (*13*). Moreover in pNET patients, serum VEGF-A levels did not differ between patients treated with everolimus or placebo (*14*). Therefore, it might be more relevant to determine the VEGF-A production at the site of the tumor lesions.

We have developed both SPECT and PET radiopharmaceuticals to visualize VEGF-A noninvasively with the VEGF-A antibody bevacizumab coupled to a radionuclide (*15*). We showed that everolimus lowered ^{89}Zr-bevacizumab uptake in an ovarian cancer xenograft model and coincided with lowered tumor VEGF-A levels (*16*). Moreover, this approach is feasible in patients. ^{111}In-bevacizumab SPECT could visualize all tumor lesions in melanoma patients (*17*). Given the superior resolution and quantification options of PET, we subsequently developed the PET tracer ^{89}Zr-bevacizumab. We showed ^{89}Zr-bevacizumab uptake in numerous tumor lesions in untreated renal cell cancer patients (*18*).

Received Jul. 23, 2013; revision accepted Jan. 3, 2014.
For correspondence or reprints contact: Elizabeth G.E. de Vries, Department of Medical Oncology, University Medical Center Groningen, P.O. Box 30,001, 9700 RB Groningen, The Netherlands.
E-mail: e.g.e.de.vries@umcg.nl
Published online May 1, 2014.

Therefore, we decided to perform a feasibility study in which we used ^{89}Zr-bevacizumab PET to investigate whether NET lesions in patients can be visualized and whether ^{89}Zr-bevacizumab tumor uptake changes during everolimus therapy.

MATERIALS AND METHODS

Patients

Patients with advanced nonresectable well-differentiated (low or intermediate grade) (*19,20*) NETs, 18 y or older with an Eastern Cooperative Oncology Group performance score of 0–2 (*21*) with adequate bone marrow and hepatic/renal function, controlled lipid profile and glucose levels, radiologic documentation of progressive disease over the past year, and measurable lesions according to the Response Evaluation Criteria in Solid Tumors, version 1.1 (RECIST1.1), were eligible (*22*). Exclusion criteria were uncontrolled medical conditions, such as unstable cardiac disease; serious infections; and any psychologic, familial, sociologic, or geographic conditions with the potential of hampering compliance with the study. The study was approved by the local Medical Ethical Committee. All participants gave written informed consent. The study is registered on clinicaltrials.gov (NCT01338090).

Everolimus Treatment and Patient Monitoring

Treatment consisted of a 10-mg dose of everolimus (orally) once daily. In the case of grade 3 toxicity, doses were reduced to 5 mg every other day. Patients were treated until disease progression based on RECIST1.1 or intolerable toxicity. Progression-free survival was defined as length of everolimus treatment until progressive disease according to RECIST1.1 or clinical progression. Before the start of everolimus, after 11 d, and every 4 wk during treatment, the patient visited the outpatient clinic for medical history, physical examination, and blood tests. Blood tests consisted of measurements of blood counts, renal and hepatic function, lipid profile, glucose, and chromogranin A. Serum chromogranin A levels were determined as described earlier (*23*). At 2 and 12 wk, everolimus levels were measured in ethylenediaminetetraacetic acid blood by liquid chromatography and tandem mass spectrometry, as described previously (*24*). At baseline and 12 wk, serum VEGF-A levels were determined with the Quantikine enzyme-linked immunosorbent assay kit (R&D Systems).

^{89}Zr-Bevacizumab PET/CT and CT

Bevacizumab (25 mg/mL; Roche) was conjugated and labeled in University Medical Center Groningen cleanroom facilities under good manufacturing practice conditions as described earlier (*16,25*). Four days before each ^{89}Zr-bevacizumab PET scan, 37 MBq of ^{89}Zr-bevacizumab (protein dose, 5 mg) were administered intravenously. Whole-body PET imaging was performed from the upper legs to the head in 6–8 bed positions of 5-min acquisition times each. All patients underwent ^{89}Zr-bevacizumab PET scanning at baseline and after 2 wk of everolimus treatment. ^{89}Zr-bevacizumab PET after 12 wk of everolimus treatment was performed only if tumor lesions could be visualized on earlier ^{89}Zr-bevacizumab PET scans. At baseline and after 12 wk, the PET scan was combined with a diagnostic CT of the chest and abdomen (Biograph mCT PET/CT, 4 detector rings, 64-slice CT; Siemens). Staging after 6 mo and every 3 mo thereafter was performed with a multislice CT scanner (Sensation 16- or 64-slice CT; Siemens). Diagnostic CT scans were obtained before and after administration of intravenous contrast agent as a triphase scan, with a maximal slice thickness of 5.0 mm.

Image and Data Analysis

The image quality of 37 MBq of ^{89}Zr provides a resolution of approximately 10 mm on PET. Therefore, the total number of tumor lesions 10 mm or greater on the baseline CT scan was determined. ^{89}Zr-bevacizumab PET was compared with the baseline CT scan. For lesions outside the field of view of the CT, other nuclear medicine imaging techniques were used for verification.

Tracer uptake was quantified in tumor lesions and organs with AMIDE Medical Image Data Examiner software (version 0.9.1; Stanford University) by drawing 3-dimensional regions of interest (*26*). Mean and maximum standardized uptake values (SUV_{mean} and SUV_{max}, respectively) were calculated. If more than 10 tumor lesions were visualized in 1 organ, then 10 were quantified. A high correlation was found between SUV_{mean} and SUV_{max} for healthy organs and tumor lesions (Pearson $r^2 = 0.99$ and 0.97, respectively, $P < 0.0001$). Because it is less operator-dependent, we present data as SUV_{max}. The difference in SUV_{max} (ΔSUV_{max}) of all tumor lesions and ΔSUV_{max} of the most intense (^{89}Zr-bevacizumab–accumulating) tumor lesion per patient were assessed after 2 and 12 wk with respect to SUV_{max} at baseline. For patients individually, correlations were analyzed between baseline SUV_{max} and ΔSUV_{max} and the percentage change in sum of target lesion diameters on CT according to RECIST1.1. ΔSUV_{max} was correlated with serum chromogranin A and VEGF-A and whole-blood everolimus concentrations.

Statistical Analyses

To be able to study our primary endpoint—a change in ^{89}Zr-bevacizumab uptake in tumor lesions between the baseline PET scan and the scans obtained after 2 and 12 wk—it was estimated that a minimum of 11 patients was needed to predict with 80% power (with 2-sided $\alpha = 0.05$) that there is a true difference in standardized uptake value ($\geq$1.25 SD) between the baseline scan and the scan after 2 and 12 wk of treatment. Therefore, the aim was to include 14 patients. The secondary endpoint was progressive disease according to RECIST1.1 on CT after 12 wk of treatment. Data are presented as median and range, unless otherwise indicated. Pearson and Spearman rank correlation served to calculate correlations of parametric and nonparametric data, respectively. The Mann–Whitney test was used for unpaired data, and the Wilcoxon signed-rank test was used for paired data. With Kaplan–Meier analysis, the progression-free survival was determined. SPSS (version 18; IBM) was used for the statistical analyses. A P value of less than 0.05 was considered statistically significant.

RESULTS

Patient Characteristics

Between April 2010 and February 2011, 14 patients were included. Patient characteristics are presented in Table 1. Six patients had serotonin-producing NETs. Five of them already received somatostatin analogs, which were continued during everolimus treatment.

Currently, 6 patients are still on everolimus, with a median treatment duration of 19 mo (range, 14–21 mo). Five patients stopped treatment because of disease progression: 1 patient each after 6, 8, and 10 mo and 2 patients after 12 mo. Two patients discontinued because of toxicity: lingual angioedema in one after 4 wk of treatment and fatigue in the other after 3 mo. One patient was lost to follow-up after 12 mo (Table 2).

All of the 13 patients evaluable for tumor response experienced stable disease according to RECIST1.1, after 3 and 6 mo. Progression-free survival at 12 mo was 64%; the median progression-free survival is not yet reached.

Baseline ^{89}Zr-Bevacizumab PET

Four days after the tracer injection, typical antibody distribution (*17,27*) of ^{89}Zr-bevacizumab was visible in healthy tissues at baseline and after 2 and 12 wk. High ^{89}Zr-bevacizumab uptake was present in the circulation (including the heart), kidneys, liver, and

TABLE 1
Baseline Patient Characteristics (n = 14)

Characteristic	*n*
Age (y)	
Median	60
Range	43–67
Sex	
Male	7
Female	7
Eastern Cooperative Oncology Group performance score	
0	12
1	1
2	1
Localization of the primary tumor	
Lung	1
Pancreas	7
Duodenal bulb	1
Small bowel	3
Unknown	2
NET World Health Organization grading	
Grade 1	8
Grade 2	6
Peptide-producing NET	
Chromogranin A producing	12
Serotonin producing	6
Gastrin producing	1
Prior treatment	
Surgery	7
Radiotherapy	3
Systemic therapy	6
Somatostatin analog	1
Interferon α	2
Chemotherapy	2
Radioactive lutetium octreotide/ metaiodobenzylguanidine	2
Sunitinib	1

spleen and low uptake in lung, muscle, bone, and brain (Supplemental Fig. 1; supplemental materials are available at http://jnm.snmjournals.org).

In 10 patients, ^{89}Zr-bevacizumab PET visualized 63 tumor lesions, and in 4 patients no tumor lesions were detected. ^{89}Zr-bevacizumab PET detected 19 lesions in the bone, 36 in the liver, 4 in the pancreas, 2 in the spleen, 1 in the bowel, and 1 mediastinal lymph node. The median number of visualized lesions per patient was 3 (range, 1–34) (Table 2), with a median SUV_{max} of 5.8 (range, 1.7–15.1). Seven lesions in 4 patients were located outside the field of view of CT. These lesions were confirmed bone metastases with other imaging techniques: 1 with ^{18}F-FDG, 3 with ^{11}C-5-hydroxytryptophan (^{11}C-5-HTP), 1 with ^{18}F-dihydroxy-phenyl-alanine PET, and 2 with ^{99m}Tc-oxidronate (bone scanning). One lesion was located in the field of view but not detected on CT: this lesion was confirmed with ^{11}C-5-HTP PET. In all patients, the baseline CT scan detected 327 lesions 10 mm or greater. In the 10 patients with tumor lesion uptake on ^{89}Zr-bevacizumab PET, 19% of lesions 10 mm or greater showed uptake on ^{89}Zr-bevacizumab PET.

Serial ^{89}Zr-Bevacizumab Tumor Uptake

In the 10 patients with a positive ^{89}Zr-bevacizumab PET scan finding, 7 showed a decrease of the tumor SUV_{max}, whereas in 3 patients the tumor SUV_{max} increased (Supplemental Fig. 2).

At a tumor lesion–based level, tumor SUV_{max} decreased during everolimus treatment, with a median of −7% at 2 wk (P = 0.09) and a median of −35% at 12 wk ($P < 0.001$) (Fig. 1). Figure 2 shows an example of serial ^{89}Zr-bevacizumab PET scans in a midgut NET patient. The change of tumor SUV_{max} was not induced by changes in tumor size, because percentage change in tumor SUV_{max} did not correlate with the percentage change in longitudinal tumor size on CT after 12 wk (r^2 = 0.072).

^{89}Zr-Bevacizumab PET Related to Treatment Outcome

The secondary objective was to explore whether ^{89}Zr-bevacizumab PET could early identify patients with progressive disease according to RECIST1.1 after 3 mo. However, none of the patients experienced progressive disease after 3 and 6 mo of everolimus treatment. Of the 4 patients without tracer uptake in tumor lesions, 3 were evaluable for response and experienced stable disease for 12 and 20+ mo, whereas 1 discontinued everolimus after 3 mo because of side effects. The 10 patients with a positive ^{89}Zr-bevacizumab PET scan finding experienced stable disease ongoing for 6–21+ mo (median, 13 mo). The 7 patients with decrease in tumor SUV_{max} experienced stable disease for 6–21+ mo (median, 16+ mo). The 3 patients with an increase in tumor SUV_{max} experienced stable disease for 8 and 12 mo, and 1 patient was lost to follow-up (Table 2).

There was no correlation between baseline tumor SUV_{max} and the percentage change in the sum of target lesion diameters on CT according to RECIST1.1 after 6 mo (Fig. 3). ΔSUV_{max} after 2 and 12 wk, however, correlated with the percentage change in the sum of the target lesion diameters according to RECIST1.1 on CT after 6 mo (r^2 = 0.51, $P < 0.05$, and r^2 = 0.61, $P < 0.01$, respectively) (Fig. 3).

^{89}Zr-Bevacizumab PET Versus Everolimus, Chromogranin A, and VEGF-A Blood Levels

Eleven patients were evaluable for whole-blood everolimus levels at 2 and 12 wk of therapy (median, 13.4 μg/L, and range, 10.3–30.3 μg/L; and median, 15.6 μg/L, and range, 6.3–30.1 μg/L, respectively) (Fig. 4). No correlation was found between everolimus levels and the change in ΔSUV_{max} at 2 and 12 wk (data not shown).

Serum VEGF-A levels were lower at 12 wk (median, 240 pg/mL; range, 16–1,220) than at baseline (median, 375 pg/mL; range, 92–1,629) (n = 13) ($P < 0.05$) (Fig. 4). Percentage change in VEGF-A serum levels after 12 wk did not correlate with change of ΔSUV_{max} after 12 wk (data not shown). Baseline median chromogranin A level was 821 μg/L (range, 66–49,700 μg/L). In patients with elevated levels (>100 μg/L), percentage change of serum chromogranin A levels after 3, 6, 9, and 12 mo did not correlate with ΔSUV_{max} after 12 wk (data not shown).

DISCUSSION

This study shows that ^{89}Zr-bevacizumab PET can visualize tumor lesions in patients with advanced well-differentiated NETs. In 10 of 14 patients, 63 tumor lesions were visible, representing 19% of the lesions 1 cm or greater on CT in these individuals. Everolimus treatment decreased ^{89}Zr-bevacizumab tumor accumulation by 7% at 2 wk (not significant) and by 35% at 12 wk. In addition, ΔSUV_{max} correlated with percentage change in tumor size of target lesions on CT at 6 mo.

The negative PET scan findings in 4 patients are remarkable, because a study with ^{111}In-bevacizumab SPECT in stage III/IV

TABLE 2
Imaging Characteristics and Treatment Outcome Per Patient (n = 14)

Tumor location	Functional NET	No. of metastases			$SUV_{mean/max}$			Treatment duration (mo)	Best change CT target lesions (%)
		CT	PET	%	Baseline	2 wk	12 wk		
Pancreas*	—	82	34	41	10.9	10.3	6.7	21+	−14
Pancreas†	—	7	0	0	—	—	—	1	NA
Pancreas	—	26	1	4	5.5	5.6	4.8	21+	−7
Pancreas	—	1	0	0	—	—	—	20+	13
Pancreas	—	39	11	31	5.1	4.5	3.6	10	−4
Pancreas	—	27	4	15	2.9	2.8	2.7	14+	−9
Pancreas	—	3	3	100	4.8	5.9	5.7	12	0
Duodenum	Gastrin	16	3	19	3.4	3.2	2.6	6	−5
Lung	Serotonin	41	3	7	7.0	7.9	9.1	8	−3
Small bowel†	Serotonin	2	0	0	—	—	—	3	11
Small bowel‡	Serotonin	29	2	7	8.5	8.8	8.8	12	1
Small bowel	Serotonin	25	0	0	—	—	—	12	−19
Unknown	Serotonin	15	1	7	10.4	8.6	7.7	18+	−9
Unknown	Serotonin	14	1	7	8.6	4.9	2.6	16+	−13

*von Hippel-Lindau germline mutation carrier.
†Taken off trial because of side effects.
‡Lost to follow-up at 12 mo.

melanoma patients and studies with ^{89}Zr-bevacizumab PET in metastatic renal cell carcinoma patients and patients with early breast cancer demonstrated tumor lesions in all but 1 breast cancer patient (*17,18,28*). Tumor VEGF-A levels were not available in the current study, because no tumor biopsies were obtained at the moment of PET scanning. In stage III/IV melanoma patients, ^{111}In-bevacizumab uptake clearly correlated with degree of VEGF-A tumor expression assessed by immunohistochemistry (*17*). In addition, in patients with primary breast cancer ^{89}Zr-bevacizumab uptake correlated with VEGF-A tumor levels measured with enzyme-linked immunosorbent assay (*28*).

The VEGF family consists of 4 different subtypes: VEGF-A, -B, -C, and -D. VEGF-A is considered to be the key player in tumor angiogenesis. VEGF-B is an inefficient factor for induction of angiogenesis. VEGF-C and -D induce venous and lymphatic angiogenesis (*29*). The involvement of different VEGF subtypes in NETs has been poorly investigated. In 50 low-grade gastrointestinal NETs, VEGF-A protein expression was strong in 32%, weak in 54%, and absent in 14% of the tumors (*3*). In 23 pNET patients, VEGF-A and -C protein expression were studied. There was a limited VEGF-A protein expression in both the primary tumor (n = 19) and the liver metastases (n = 7). Although VEGF-C expression was limited in primary tumors, liver metastases did show high expression (*30*). In another study, expression of all VEGF subtypes was quantified with real-time polymerase chain reaction in 25 patients with ileal NETs. VEGF-A expression was similar between tumor lesions and healthy ileal mucosa. In contrast, VEGF-B and VEGF-D levels were higher in tumors than in normal mucosa (*31*). This might explain why several of the NET lesions in our study did not show uptake of ^{89}Zr-bevacizumab.

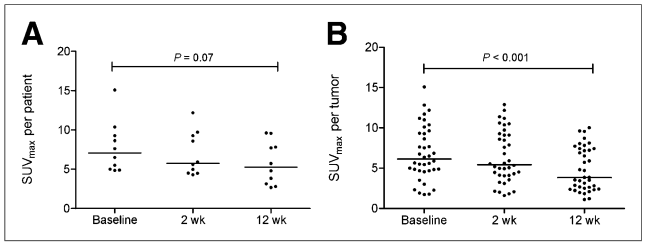

FIGURE 1. SUV_{max} in most intense tumor lesion per patient (A) and in all tumor lesions (B) at baseline, 2 wk, and 12 wk. Horizontal bars represent median values.

The heterogeneous baseline ^{89}Zr-bevacizumab PET results may be an explanation for the fact that not all NET patients benefit from antiangiogenic treatment with bevacizumab (*32–34*). It might be of interest to perform a trial with ^{89}Zr-bevacizumab PET before bevacizumab therapy to determine whether this PET scan could be useful in the selection of NET patients up front. In that case, ^{89}Zr-bevacizumab PET can be used to visualize the presence of the drug target. However, in the current study we were interested in visualizing VEGF-A as an early read out of a downstream effect of mTOR inhibition, which might give insight into the effect of treatment.

mTOR inhibition has pleiotropic antitumor effects, including reduction of tumor VEGF-A production. In the current study, we did indeed find reduced ^{89}Zr-bevacizumab tumor uptake after 2 and 12 wk of everolimus treatment. Serial imaging results are in concordance with an ovarian cancer xenograft study, in which 2 wk of everolimus treatment decreased ^{89}Zr-bevacizumab tumor uptake by 21.7% ± 4% and corresponded with lower tumor VEGF-A protein levels and microvessel density in treated animals (*16*). Not all patients with a positive ^{89}Zr-bevacizumab PET scan finding before everolimus treatment showed a reduction in tumor uptake during everolimus treatment. This differential effect was not due to inadequate everolimus levels, because in all patients the levels were comparable to those reported earlier in a phase 1 study (*35*). A negative ^{89}Zr-bevacizumab PET scan finding did not preclude benefit from treat-

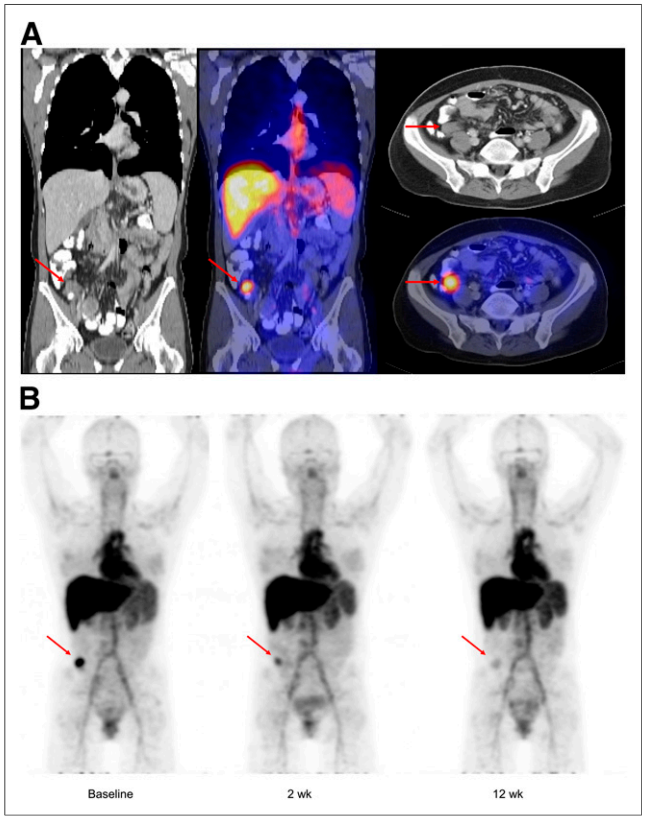

FIGURE 2. PET images 4 d after ^{89}Zr-bevacizumab injection in patient with metastatic midgut carcinoid. (A) Coronal and axial images of low-dose CT and fusion images of PET. Low-dose CT shows increased tracer uptake in abdominal tumor lesion. (B) Coronal PET images at baseline, 2 wk, and 12 wk of everolimus treatment. Physiologic ^{89}Zr-bevacizumab uptake is present in heart (blood pool), liver, spleen, and circulation. At baseline, increased ^{89}Zr-bevacizumab uptake was found in tumor lesion located in ileocecal angle (arrows). Tumor uptake was 43% lower at 2 wk and 69% lower at 12 wk during everolimus treatment.

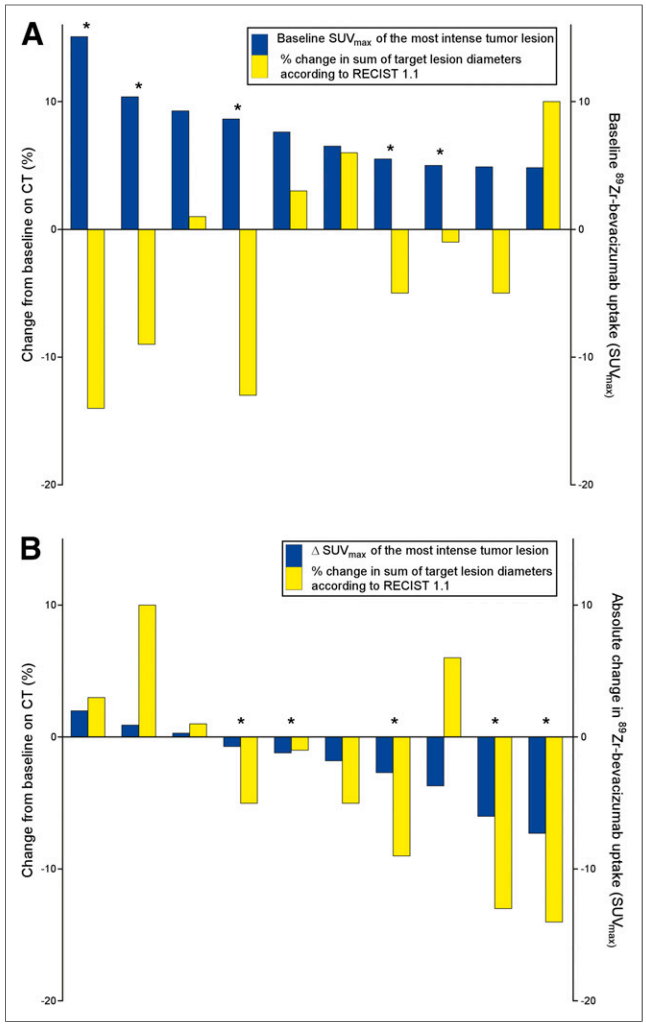

FIGURE 3. Waterfall plots of 10 patients with visualized tumor lesions at ^{89}Zr-bevacizumab PET. (A) Maximum baseline SUV_{max} (blue bars) and percentage change in sum of target lesion diameters according to RECIST1.1 on CT after 6 mo (yellow bars). (B) ΔSUV_{max} at 12 wk of most intense tumor lesion at baseline (blue bars) and percentage change in sum of target lesion diameters according to RECIST1.1 on CT after 6 mo (yellow bars). * = patient is still on everolimus.

ment with everolimus, possibly likely due to other antitumor effects of everolimus than reduction of VEGF-A.

Serum VEGF-A levels were 25% lower after 12 wk of everolimus treatment than at baseline. In the RADIANT-3 study, serum VEGF-A levels were determined at baseline and 4, 8, and 12 wk and did not change in pNET patients who received everolimus (n = 207) or placebo (n = 203) (*14*). These discrepant results may be the consequence of different assays. We observed no correlation between change in serum VEGF-A levels and tumor ΔSUV_{max} after 2 and 12 wk, suggesting that change in circulating VEGF-A does not reflect change of VEGF-A at the tumor level. This result may be explained by the fact that VEGF-A consists of different isoforms. VEGF-A_{121} and VEGF-A_{165} can diffuse freely, whereas VEGF-A_{189} and VEGF-A_{206} are attached to the extracellular matrix (*36*). Moreover, serum VEGF-A levels contain VEGF-A released by platelets (*37*).

Another useful imaging strategy to predict everolimus efficacy might be functional imaging with MR imaging, including diffusion-weighted (DW) MR imaging and contrast-enhanced MR imaging. Tumor necrosis results in increased water permeability, which can be measured by DW MR imaging. Contrast-enhanced MR imaging can quantify changes in tumor vascularity. In a retrospective study in 71 patients with advanced NETs who underwent intraarterial chemoembolization of liver metastases, DW MR imaging and contrast-enhanced MR imaging scans were obtained at baseline and 4 wk after therapy. The authors concluded

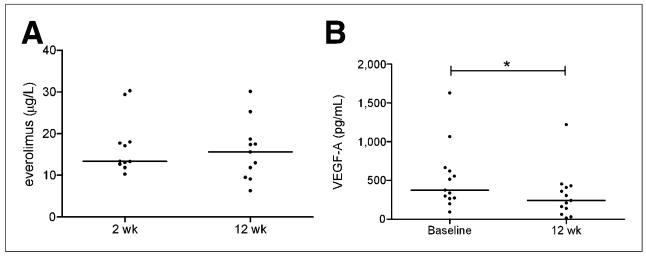

FIGURE 4. Graphs showing whole-blood everolimus levels after 2 wk and 12 wk of everolimus treatment (n = 11) (A) and serum VEGF-A levels measured at baseline and 12 wk of treatment (n = 13) (B). Horizontal bars represent median values. *$P < 0.05$.

that volumetric functional MR imaging criteria may act as biomarkers of early response (*38*). An advantage of MR imaging is that it does not expose patients to radiation.

CONCLUSION

This study demonstrates differences in ^{89}Zr-bevacizumab tumor accumulation between and within patients with advanced well-differentiated NETs. This heterogeneity likely reflects differential VEGF-A pathway activity. Everolimus treatment reduced ^{89}Zr-bevacizumab tumor accumulation without affecting normal organ distribution. A baseline ^{89}Zr-bevacizumab PET scan cannot be used to select patients for everolimus treatment. Larger studies are needed to determine the predictive value of serial scans for efficacy of everolimus treatment, but a read out of other downstream effects of mTOR inhibition might be more relevant in NETs.

DISCLOSURE

The costs of publication of this article were defrayed in part by the payment of page charges. Therefore, and solely to indicate this fact, this article is hereby marked "advertisement" in accordance with 18 USC section 1734. This study was supported by a research grant of Novartis, The Netherlands. No other potential conflict of interest relevant to this article was reported.

REFERENCES

1. Hanahan D, Weinberg RA. Hallmarks of cancer: the next generation. *Cell.* 2011;144:646–674.
2. Dong M, Phan AT, Yao JC. New strategies for advanced neuroendocrine tumors in the era of targeted therapy. *Clin Cancer Res.* 2012;18:1830–1836.
3. Zhang J, Jia Z, Li Q, et al. Elevated expression of vascular endothelial growth factor correlates with increased angiogenesis and decreased progression-free survival among patients with low-grade neuroendocrine tumors. *Cancer.* 2007;109:1478–1486.
4. Hobday TJ, Rubin J, Goldberg R, Erlichman C, Lloyd R. Molecular markers in metastatic gastrointestinal neuroendocrine tumors [abstract]. *Proc Am Soc Clin Oncol.* 2003;22:1078.
5. Terris B, Scoazec JY, Rubbia L, et al. Expression of vascular endothelial growth factor in digestive neuroendocrine tumours. *Histopathology.* 1998;32:133–138.
6. von Marschall Z, Scholz A, Cramer T, et al. Effects of interferon alpha on vascular endothelial growth factor gene transcription and tumor angiogenesis. *J Natl Cancer Inst.* 2003;95:437–448.
7. Meric-Bernstam F, Gonzalez-Angulo AM. Targeting the mTOR signaling network for cancer therapy. *J Clin Oncol.* 2009;27:2278–2287.
8. Raymond E, Dahan L, Raoul JL, et al. Sunitinib malate for the treatment of pancreatic neuroendocrine tumors. *N Engl J Med.* 2011;364:501–513.
9. Yao JC, Shah MH, Ito T, et al. RAD001 in advanced neuroendocrine tumors, Third (RADIANT-3) Study Group: everolimus for advanced pancreatic neuroendocrine tumors. *N Engl J Med.* 2011;364:514–523.
10. Pavel ME, Hainsworth JD, Baudin E, et al. Everolimus plus octreotide long-acting repeatable for the treatment of advanced neuroendocrine tumours associated with carcinoid syndrome (RADIANT-2): a randomised, placebo-controlled, phase 3 study. *Lancet.* 2011;378:2005–2012.
11. Villaume K, Blanc M, Gouysse G, et al. VEGF secretion by neuroendocrine tumor cells is inhibited by octreotide and by inhibitors of the PI3K/AKT/mTOR pathway. *Neuroendocrinology.* 2010;91:268–278.
12. Thomas GV, Tran C, Mellinghoff IK, et al. Hypoxia-inducible factor determines sensitivity to inhibitors of mTOR in kidney cancer. *Nat Med.* 2006;12:122–127.
13. Shojaei F. Anti-angiogenesis therapy in cancer: current challenges and future perspectives. *Cancer Lett.* 2012;320:130–137.
14. Yao JC, Tsuchihashi Z, Panneerselvam A, Winkler RE, Bugarini R, Pavel M. Effect of everolimus treatment on markers of angiogenesis in patients with advanced pancreatic neuroendocrine tumours (pNET): results from the phase III RADIANT-3 study [poster]. *Eur J Cancer.* 2011;47:S463.
15. Nagengast WB, de Vries EG, Hospers GA, et al. In vivo VEGF imaging with radiolabeled bevacizumab in a human ovarian tumor xenograft. *J Nucl Med.* 2007;48:1313–1319.
16. van der Bilt AR, Terwisscha van Scheltinga AG, Timmer-Bosscha H, et al. Measurement of tumor VEGF-A levels with ^{89}Zr-bevacizumab PET as an early biomarker for the antiangiogenic effect of everolimus treatment in an ovarian cancer xenograft model. *Clin Cancer Res.* 2012;18:6306–6314.
17. Nagengast WB, Lub-de Hooge MN, van Straten EM, et al. VEGF-SPECT with ^{111}In-bevacizumab in stage III/IV melanoma patients. *Eur J Cancer.* 2011;47:1595–1602.
18. Oosting SF, Brouwers AH, van Es SC, et al. ^{89}Zr-bevacizumab PET imaging in metastatic renal cell carcinoma patients before and during antiangiogenic treatment [abstract]. *J Clin Oncol.* 2012;30(May 20 suppl):10581.
19. Rindi G, Klöppel G, Alhman H, et al. TNM staging of foregut (neuro)endocrine tumors: a consensus proposal including a grading system. *Virchows Arch.* 2006;449:395–401.
20. Rindi G, Klöppel G, Coulevard A, et al. TNM staging of midgut and hindgut (neuro) endocrine tumors: a consensus proposal including a grading system. *Virchows Arch.* 2007;451:757–762.
21. Oken MM, Creech RH, Tormey DC, et al. Toxicity and response criteria of the Eastern Cooperative Oncology Group. *Am J Clin Oncol.* 1982;5:649–655.
22. Eisenhauer EA, Therasse P, Bogaerts J, et al. New response evaluation criteria in solid tumours: revised RECIST guideline (version 1.1). *Eur J Cancer.* 2009;45:228–247.
23. Fiebrich HB, de Jong JR, Kema IP, et al. Total ^{18}F-DOPA PET tumour uptake reflects metabolic endocrine tumour activity in patients with a carcinoid tumour. *Eur J Nucl Med Mol Imaging.* 2011;38:1854–1861.
24. Koster RA, Dijkers ECF, Uges DRA. Robust, high-throughput LC-MS/MS method for therapeutic drug monitoring of cyclosporine, tacrolimus, everolimus and sirolimus in whole blood. *Ther Drug Monit.* 2009;31:116–125.
25. Verel I, Visser GW, Boellaard R, Stigter-van Walsum M, Snow GB, van Dongen GA. ^{89}Zr immuno-PET: comprehensive procedures for the production of ^{89}Zr-labeled monoclonal antibodies. *J Nucl Med.* 2003;44:1271–1281.
26. Loening AM, Gambhir SS. AMIDE: a free software tool for multimodality medical image analysis. *Mol Imaging.* 2003;2:131–137.
27. Dijkers EC, Oude Munnink TH, Kosterink JG, et al. Biodistribution of ^{89}Zr-trastuzumab and PET imaging of HER2-positive lesions in patients with metastatic breast cancer. *Clin Pharmacol Ther.* 2010;87:586–592.
28. Gaykema SB, Brouwers AH, Lub-de Hooge MN, et al. ^{89}Zr-bevacizumab PET imaging in primary breast cancer. *J Nucl Med.* 2013;54:1014–1018.
29. Li X, Eriksson U. Novel VEGF family members: VEGF-B, VEGF-C and VEGF-D. *Int J Biochem Cell Biol.* 2001;33:421–426.
30. Hansel DE, Rahman A, Hermans J, et al. Liver metastases arising from well-differentiated pancreatic endocrine neoplasms demonstrate VEGF-C expression. *Mod Pathol.* 2003;16:652–659.
31. Besig S, Voland P, Baur DM, Perren A, Prinz C. Vascular endothelial growth factors, angiogenesis, and survival in human ileal enterochromaffin cell carcinoids. *Neuroendocrinology.* 2009;90:402–415.
32. Yao JC, Phan A, Hoff PM, et al. Targeting vascular endothelial growth factor in advanced carcinoid tumor: a random assignment phase II study of depot octreotide with bevacizumab and pegylated interferon α-2b. *J Clin Oncol.* 2008;26:1316–1323.
33. Kulke MH, Chan JA, Meyerhardt JA, et al. A prospective phase II study of 2-methoxyestradiol administered in combination with bevacizumab in patients with metastatic carcinoid tumors. *Cancer Chemother Pharmacol.* 2011;68:293–300.
34. Chan JA, Stuart K, Earle CC, et al. Prospective study of bevacizumab plus temozolomide in patients with advanced neuroendocrine tumors. *J Clin Oncol.* 2012;30:2963–2968.
35. O'Donnell A, Faivre S, Burris HA 3rd, et al. Phase I pharmacokinetic and pharmacodynamic study of the oral mammalian target of rapamycin inhibitor everolimus in patients with advanced solid tumors. *J Clin Oncol.* 2008;26:1588–1595.
36. Park JE, Keller GA, Ferrara N. The vascular endothelial growth factor (VEGF) isoforms: differential deposition into the subepithelial extracellular matrix and bioactivity of extracellular matrix-bound VEGF. *Mol Biol Cell.* 1993;4:1317–1326.
37. Jelkmann W. Pitfalls in the measurement of circulating vascular endothelial growth factor. *Clin Chem.* 2001;47:617–623.
38. Gowdra Halappa V, Corona-Villalobos CP, Bonekamp S, et al. Neuroendocrine liver metastases treated by using intraarterial therapy: volumetric functional imaging biomarkers of early tumor response and survival. *Radiology.* 2013;266:502–513.

The Journal of NUCLEAR MEDICINE

Everolimus Reduces ^{89}Zr-Bevacizumab Tumor Uptake in Patients with Neuroendocrine Tumors

Sophie J. van Asselt, Sjoukje F. Oosting, Adrienne H. Brouwers, Alfons H.H. Bongaerts, Johan R. de Jong, Marjolijn N. Lub-de Hooge, Thijs H. Oude Munnink, Helle-Brit Fiebrich, Wim J. Sluiter, Thera P. Links, Annemiek M.E. Walenkamp and Elisabeth G.E. de Vries

J Nucl Med. 2014;55:1087-1092.
Published online: May 1, 2014.
Doi: 10.2967/jnumed.113.129056

The Journal of Nuclear Medicine is published monthly.
SNMMI | Society of Nuclear Medicine and Molecular Imaging
1850 Samuel Morse Drive, Reston, VA 20190.
(Print ISSN: 0161-5505, Online ISSN: 2159-662X)

SNMMI SOCIETY OF NUCLEAR MEDICINE AND MOLECULAR IMAGING